Temporal resolution calibration of a single-shot autocorrelator by a picosecond pulse

Yang Wang (王 杨)[1], Xiaoping Ouyang (欧阳小平)[1,*], Haitang Qin (秦海棠)[1], Daizhong Liu (刘代中)[1], Dong Yang (杨 冬)[1], Lin Yang (杨 琳)[1], Baoqiang Zhu (朱宝强)[1], Jian Zhu (朱 俭)[2], and Jianqiang Zhu (朱健强)[1]

[1]*Joint Laboratory on High Power Laser and Physics, Shanghai Institute of Optics and Fine Mechanics, Chinese Academy of Sciences, Shanghai 201800, China*

[2]*Shanghai Institute of Laser Plasma, China Academy of Engineering Physics, Shanghai 201800, China*

**Corresponding author: oyxp@siom.ac.cn*

Received March 30, 2015; accepted May 10, 2015; posted online October 13, 2015

A new method is proposed to deduce the temporal resolution of a single-shot autocorrelator. A resolution test pattern is installed in one arm of the autocorrelator to add streaks on the beam cross section. Therefore, the autocorrelation signal is modulated when the streaked beam arrives at an autocorrelation crystal. Given the relationship between streak width and temporal delay in an autocorrelator, the temporal resolution is determined by the noncollinear angle, the streak's width of the resolution test pattern, and the autocorrelation signal. Comparison experiments show that the proposed and conventional calibration schemes yield temporal resolutions of 65.6 and 67.8 fs/pixel, respectively, with a relative error of 3.3%. An advantage of this method is that fine temporal resolution (65.6 fs/pixel) is achievable on a short pulse (10 ps) despite the lack of a femtosecond pulse.

OCIS codes: 140.7090, 320.7080, 320.7100, 170.3600.
doi: 10.3788/COL201513.S21407.

With the development of high-power lasers, high-energy petawatt laser facilities with picosecond pulses have been widely applied in high-energy-density physics, as well as in fast ignition and advanced radiography capability. Picosecond diagnostics systems are used to obtain the parameters (e.g., energy, pulse width, far-field, pulse contrast, and spectrum) of picosecond petawatt laser facilities[1,2]. Single-shot autocorrelators have been used to determine the pulse widths of picosecond pulses in recent years. Janszky has theoretically analyzed the autocorrelation function to determine the pulse widths of ultrafast pulses[3]. Autocorrelation is widely used to measure the pulse width of ultrashort pulses[4–8].

Before the measurement of pulse width, the temporal resolution calibration experiment is essential for every autocorrelator. Temporal resolution has historically been calculated as per theory, and verified through a self-calibration experiment. In the self-calibration method, the autocorrelator is calibrated by the measured pulse itself[6,9]. Each delay time corresponds to a different peak position. It is not difficult to identify the pulse width.

In order to analyze pulse widths ranging from 500 fs to 10 ps on a 1-kJ laser[10], an autocorrelator is required, and is to be based initially on an approximately 10-ps laser. The tolerance of a conventional scheme will be too large to measure a 500-fs pulse precisely when it is calibrated by an approximately 10-ps pulse. To deduce the temporal resolution of an autocorrelator in this case, this Letter provides a geometric method to describe the relationship between the spatial intensity distribution and pulse width in autocorrelation generation. This new scheme can achieve high precision on an approximately 10-ps laser pulse despite the lack of a femtosecond pulse.

Autocorrelation involves two incident pulses with the same temporal shape and intensity distribution. A Gaussian function is used to describe the temporal shape of the ultrafast pulse. Hence, the measured pulse is divided into two parts, $I_1(t)$ and $I_2(t)$, given as

$$I_1(t) = I_2(t) = \exp\left(-4\ \ln 2 \frac{t^2}{\Delta T^2}\right), \tag{1}$$

where ΔT is the pulse width of the input pulse, I is the intensity, and t is time.

Autocorrelation is generated after the two pulses pass through a nonlinear crystal. The autocorrelation signal $A(\tau)$ is expressed as

$$A(\tau) = \int I_1(t) I_2(t-\tau) \mathrm{d}t, \tag{2}$$

where τ is the time delay between two optical arms in the autocorrelator. Hence, Eq. (2) is rewritten as

$$A(\tau) = \exp\left(-4\ \ln 2 \frac{\tau^2}{\Delta T_A^2}\right), \tag{3}$$

where ΔT_{A} is the full-width at half-maximum (FWHM) of the autocorrelation signal, and is obtained by a detector. Moreover, as per Ref. [8], $\Delta T_A = \sqrt{2} \cdot \Delta T$.

Figure 1 shows a schematic of a single-shot autocorrelator, in which the measured pulse is divided into two parts by a beam splitter. The transmitted part goes through Mirror $\mathrm{M_1}$ and reaches an autocorrelation generator (ACG). A nonlinear crystal of β–$\mathrm{BaB_2O_4}$ is used in the

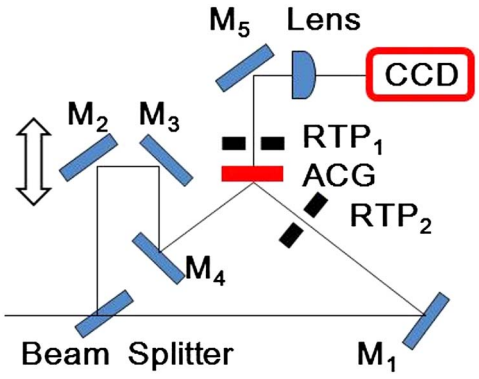

Fig. 1. Schematic of a single-shot autocorrelator.

ACG. And its thickness is 1 mm. The reflected part goes through an optical path delayer that is comprised of Mirrors M_2 and M_3 located 90° to each other, then reflected by Mirror M_4, and finally reaches the ACG as well. The two pulses simultaneously arrive at the ACG by adjusting the optical path delayer. Resolution test patterns (RTPs) RTP_1 and RTP_2 are used for subsequent experiments on the temporal resolution.

Figure 2 shows a schematic of the temporal resolution experiment, in which the ACG is the front surface of the autocorrelation crystal. Solid and dashed lines correspond to the first and second beam arm, respectively, during autocorrelation. The equal phase plane (EFP) is a set of all points with equal optical paths to Point O in each beam arm. When the center beamlet of the first and second beam arm simultaneously arrive at the autocorrelation surface of the ACG (the plane with Line Segment AO), the interaction time between the two pulses are longest at Point O and equal to the entire pulse width. Hence, the peak of the correlation signal is located at Point O.

As shown in Fig. 2, L_{1A} is the optical distance that the right-edge beamlet of the first beam arm traverses to arrive at Point A on the ACG plane. Term L_{1O} represents the optical distance that the center beamlet of first beam arm traverses to arrive at Point O on the ACG plane. Furthermore, $L_{1A} < L_{1O}$ at the $-z$ axis, and L_{2A} is the optical distance that the right-edge beamlet of the second beam arm traverses to arrive at Point A on the ACG

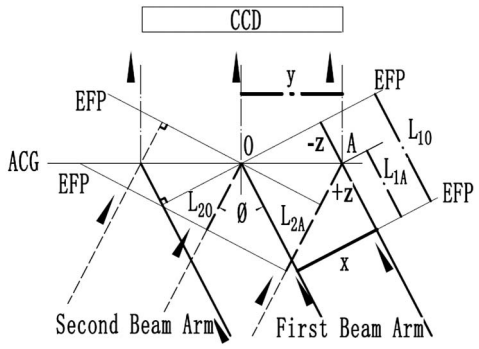

Fig. 2. Schematic of the temporal resolution experiment in a single-shot autocorrelator.

plane. Finally, L_{2O} is the optical distance that the center beamlet of the second beam arm traverses to arrive at Point O on the ACG plane. The value of L_{2A} is larger than L_{2O} at the $+z$ axis. Hence, the distances can be expressed as

$$L_{1O} - z = L_{1A}, \tag{4}$$

$$L_{2O} + z = L_{2A}, \tag{5}$$

$$L_{1O} = L_{2O}. \tag{6}$$

The peak of the autocorrelation signal shifts from Point O to Point A via the traditional method during the movement of the optical path delay[6]. The signal movement is denoted as y, and L_{2A} is changed to L'_{2A} such that $L'_{2A} = L_{1A}$. Equations (4)–(6) yield the expression for L'_{2A}, as

$$L'_{2A} = L_{2A} - 2z. \tag{7}$$

Hence, the movement of the optical path delay is $2z$ and the time variation is $\Delta t = 2z/\mathrm{c}$. Term c is the velocity of light. The relationship between the movement of signal peak y and time variation Δt are expressed as

$$\rho = \frac{\Delta t}{y} = \frac{2z}{cy}, \tag{8}$$

where ρ is a temporal resolution in the self-calibration experiments.

In our work, a new scheme is proposed by installing an RTP in the first beam arm. Streaks with specific sizes on the RTP are expressed as x. Figure 2 reveals that peak movement y of the autocorrelation signal with optical distance z and streak width x forming a right-triangle. The relationship between x and y is given as

$$y = \frac{x}{\cos\left(\frac{\varphi}{2}\right)}, \tag{9}$$

where φ is the noncollinear angle between the two beam arms. Along the direction of beam propagation, the relationship between x and z is

$$z = x \tan\left(\frac{\varphi}{2}\right). \tag{10}$$

Therefore, ρ is derived from Eqs. (8)–(10)

$$\rho = \frac{2z}{cy} = \frac{2x \tan\left(\frac{\varphi}{2}\right)}{cy}. \tag{11}$$

Equation (11) shows that the width x of the RTP and φ can be measured prior to the experiment, where c is as defined previously. The peak of the autocorrelation signal remains stationary in the proposed scheme. Hence, y represents a virtual movement in our work and can be obtained by photoelectric detectors, such as a CCD. Peak movements of the autocorrelation signal are not

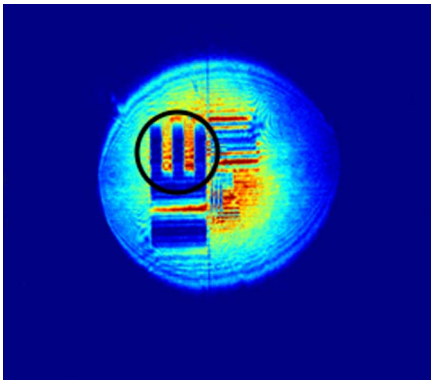

Fig. 3. CCD image from RTP_1.

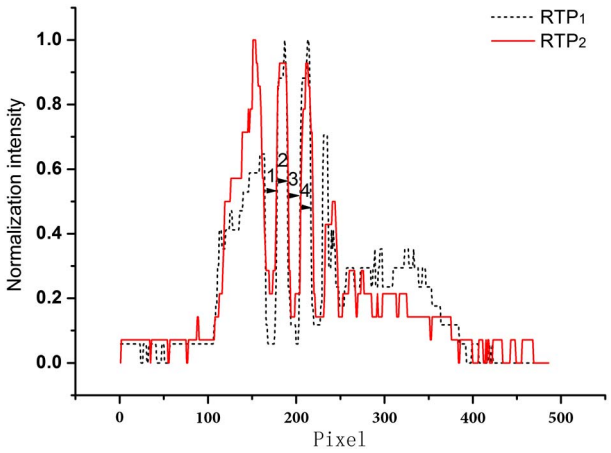

Fig. 4. Streaks in CCD image y_{CCD} from RTP_1 and RTP_2.

necessary, and no special requirements are imposed on the pulse width.

Figure 1 shows the autocorrelator setup, in which ρ is determined by a laser with a pulse-width of approximately 10 ps based on a scanning autocorrelator. A cylinder lens is installed between the ACG and the photoelectric detector (i.e., the CCD). The autocorrelation signal is recorded on the CCD to improve the precision and accuracy by suppressing the diffraction of small structures. Finally, data analysis is performed by a computer.

An RTP is placed behind the ACG at the position of RTP_1 (Fig. 1), and the magnification of the optical imaging system is calculated. The resultant CCD image is shown in Fig. 3. Threadlike streaks are blurred because of diffraction. Fortunately, streaks of 250 μm are clear. The width of each bright or dark streak is measured by pixels. The pixel size of our CCD is 20 μm × 20 μm. A comparison of the manufacturing width of the RTP yielded a magnification $M = 1.04$ from Table 1.

Subsequently, the RTP is changed from RTP_1 to RTP_2 (Fig. 2), and the pattern should be as close to the ACG as possible. The distance between RTP_2 and the ACG is 10 mm because of a slant angle. Figure 4 shows the corresponding results of y_{CCD} each position. There is an approximately 2-pixel translation of the third dark fringe; we primarily attribute this to a slant angle and lens aberration for RTP_2. In order to reduce the calculation error, four streaks (1–4) with a clear edge are selected.

Table 1. Magnification of RTP_1 Imaged on a CCD

Item	Manufacturing Size of RTP x (μm)	Width of Streak in CCD Image y_{CCD} at RTP_1 (pixels)	Magnification of RTP_1
1	—	13	1.04
2	—	12.5	1
3	—	14	1.12
4	—	12.5	1
Average	250	13	1.04
RMS error (%)	δ_x	5.44	$\delta_M = 5.44$

Given the width of each bright or dark streak and magnification M of the cylindrical lens, the virtual movement of the ACG peak signal is

$$y = \frac{y_{CCD}}{M} \times 20\ \mu\text{m/pixel}, \tag{12}$$

where ρ was calculated from Eqs. (11) and (12). Data is averaged over four distinct measurements (Table 2) to reduce uncertainty.

From Eq. (12), the RMS error of y should be

$$\delta_y = \sqrt{\delta_M^2 + \delta_{y_{CCD}}^2}. \tag{13}$$

where δ_y is RMS of y , δ_M is RMS error of M, and $\delta_{y_{CCD}}$ is RMS error of y_{CCD}.

We can find from Tables 1 and 2 that the width of bright and dark streaks fluctuate. This is caused by the diffraction effect and lens aberration.

We analyze the uncertainty of the calculated values of ρ with Table 1 and Table 2. The value of x of the RTP is ensured by manufacturing with an absolute error of ±2 μm. For a picosecond autocorrelator with $x = 250$ μm, the uncertainty in x is equal to $\delta_x = \pm 0.8\%$.

Term φ is measured by a combination square, in which its absolute error is $< \pm 1°$. For this picosecond autocorrelator, $\varphi = 55°$ and its uncertainty is found to be 2.13%.

The systemic uncertainty in temporal resolution of the picosecond autocorrelator is

$$\begin{aligned}\delta &= \sqrt{\delta_x^2 + \delta_{\tan(\frac{\varphi}{2})}^2 + \delta_y^2} \\ &= \sqrt{0.8^2 + 2.13^2 + 5.44^2 + 1.82^2} = 6.17\%.\end{aligned} \tag{14}$$

The temporal resolution is 65.6 fs/pixel as per this new method (Table 2). This method gives results that are close to the theoretical values.

The temporal resolution ρ is also deduced on approximately 180 fs pulses for comparative purposes (Fig. 5). In

Table 2. Results of Temporal Resolution Experiments[a]

Item	Manufacturing Size of RTP x (μm)	Value of Noncollinear Angle φ	Width of Streak in CCD Image y_{CCD} at RTP_2 (pixels)	Virtual Offset of Autocorrelation Signal Peak y (μm)	Temporal Resolution ρ (fs/pixel)
1	—	$\tan(55°/2)$	13.5	259.62	—
2	—	$\tan(54°/2)$	14	269.23	—
3	—	$\tan(56°/2)$	13.5	259.62	—
4	—	$\tan(55°/2)$	14	269.23	—
Average	250	0.52	13.75	264.43	65.6
RMS error (%)	δ_x	$\delta_{\tan(\varphi/2)} = 2.13$	$\delta_{y_{\mathrm{CCD}}} = 1.82$	$\delta_y = 5.74$	—

[a]$M = 1.04$.

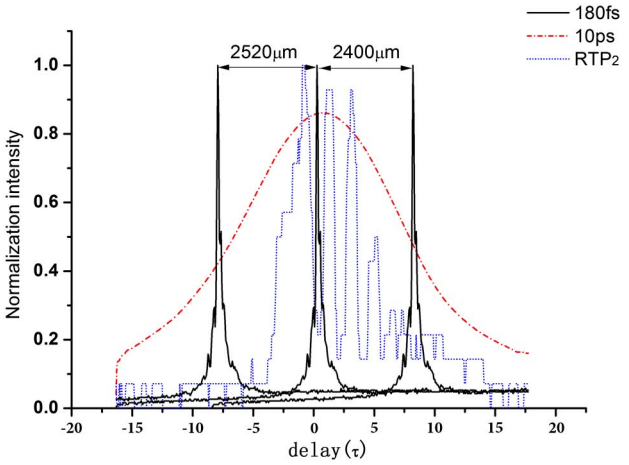

Fig. 5. Autocorrelation curve of the picosecond autocorrelator. Dashed line, results for the approximately 180-fs laser; dotted line, results for the approximately 10-ps laser; solid line, results from RTP_2.

this context, the movement of the signal peak y is 126 pixels (2520 μm) and 120 pixels (2400 μm) when the optical path delay z is 1250 μm in both cases. The value of ρ is 67.8 fs/pixel on average from Eq. (8). Moreover, the relative uncertainty between the two methods is 3.3%. The results reveal that ρ obtained from this new method is close to that of the traditional method under a femtosecond laser.

Regarding the petawatt laser of 1 kJ and 0.5–10 ps that is under construction at the Shenguang II (SGII) facility[10], diagnostics is used to analyze its performance[11]. After test experiments, the autocorrelator is set up into the diagnostics. Experimental data for the petawatt laser at the SGII facility is shown in Fig. 6. Pulse widths of 7.3, 3.0, and 0.41 ps are readily identified.

This Letter presents a new method to deduce the temporal resolution of an autocorrelator. In this new method, the autocorrelator is identified on approximately 10 ps pulses, and can then be used to analyze pulses ranging from 500 fs to 10 ps. In our work, a temporal resolution of 65.6 fs/pixel is obtained by this new method on approximately 10-ps pulses, which is sufficiently close to

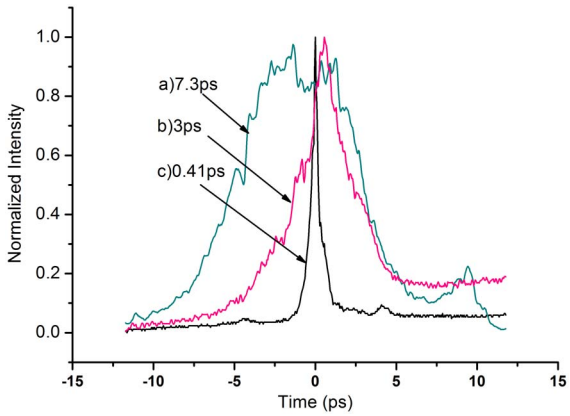

Fig. 6. Measurements for a petawatt laser at the SGII facility; Curve a, 0.41 ps (185.8 J); Curve b, 3.0 ps (111.5 J); and Curve c, 7.3 ps (3 J).

that of the traditional self-calibration method on an approximately 180-fs laser. Consequently, it is an alternate method of identifying the temporal resolution of a single-shot autocorrelator despite the lack of a femtosecond pulse. The uncertainty between the two methods is found to be 3.3%. The proposed scheme was verified and proven by experiments. This autocorrelator works well on the petawatt laser at the SGII facility.

The authors gratefully acknowledge Professor Lijia Qian for the ~180 fs laser. This work was supported by the National Natural Science Foundation of China under Grant No. NSFC-11204330.

References

1. J. D. Zuegel, S.-W. Bahk, J. Bromage, C. Dorrer, R. Earley, T. J. Kessler, B. J. Kruschwitz, S. F. B. Morse, D. N. Maywar, J. B. Oliver, J. Qiao, A. L. Rigatti, A. W. Schmid, M. J. Shoup III, L. J. Waxer, and J. H. Kelly, Rev. Laser Eng. **37**, 437 (2009).
2. Y. Kitagawa, H. Fujita, R. Kodama, H. Yoshida, S. Matsuo, T. Jitsuno, T. Kawasaki, H. Kitamura, T. Kanabe, S. Sakabe, K. Shigemori, N. Miyanaga, and Y. Izawa, IEEE J. Quantum Electron. **40**, 281 (2004).
3. J. Janszky and G. Corradi, Opt. Commun. **23**, 293 (1977).
4. Y. Ishida and T. Yajima, Opt. Commun. **56**, 57 (1985).

5. F. Salin, P. Georges, G. Roger, and A. Brun, Appl. Opt. **26**, 4528 (1987).
6. A. Brun, P. Georges, G. Le Saux, and F. Salin, J. Phys. D Appl. Phys. **24**, 1225 (1991).
7. R. A. Ganeev, F. Sh. Ganikhanov, I. G. Gorelik, A. A. Dakhin, D. G. Kunin, T. Usmanov, and A. V. Zinoviev, Opt. Commun. **114**, 432 (1995).
8. M. Raghuramaiah, A. K. Sharma, P. A. Naik, P. D. Gupta, and R. A. Ganeev, Sadhana **26**, 603 (2001).
9. G. Priebe, K. A. Janulewicz, V. I. Redkorechev, J. Tummler, and P. V. Nickles, Opt. Commun. **259**, 848 (2006).
10. T. Wang, G. Xu, Y. Dai, Z. Lin, and J. Zhu, "Recent progress on the PW beamline for SG-II-U laser facility,"in *CLEO* 1, INSPEC Accession Number: 12134535 (2011).
11. X. Ouyang, L. Yang, P. Yonghua, M. Chen, J. Ma, Y. Wang, S. Tang, C. Liu, H. Li, Y. Wang, L. Qian, J. Zhu, B. Zhu, and J. Zhu, Chin. J. Lasers **40**, 0108003 (2013).